

The Effect of T -stress on Crack Tip Plastic Zones under Mixed Mode Loading Conditions

Qays Nazarali, Xin Wang and Robert Bell

*Department of Mechanical and Aerospace Engineering, Carleton University,
Ottawa, Ontario, Canada, K1S 5B6*

ABSTRACT

In this paper we examined the influence of T -stress on crack tip plastic zones under mixed mode I and mode II loading conditions. The crack-tip stress field is defined in terms of the mixed mode stress intensity factors (SIFs) and the T -stress using the William's series expansion. The crack-tip stress field is incorporated into the Von Mises yield criteria to develop an expression that models the crack-tip plastic zone. Using the obtained plastic zone expression, the plastic zone is mapped and analyzed for various combinations of mode II to mode I SIF ratios and T -stress. The properties of plastic zone affected by T -stress are discussed.

1. INTRODUCTION

The knowledge of plastic zone size and its variation around the crack tip is important in fracture analysis of cracked specimens. Conventional estimations of plastic zone size have been made based on the crack tip stress field using the William's series expansion, and assuming the stress intensity factor K alone (i.e. the first term in the expansion) fully characterizes the stress field.

However, it has been realised the T -stress, the second term in William's series expansion plays an important role on the crack tip plastic zone size. Under pure mode I conditions, it has been shown that T -stress will change the plastic zone size significantly [1]. A positive T -stress strengthens the triaxial stress state at the crack-tip and results in a smaller plastic zone, while negative T -stress leads to the opposite i.e. a larger plastic zone. Therefore, the T -stress has been used to characterize the effect of constraint on the triaxial stress state near the crack-tip [2, 3].

The majority of research on T -stress effects has been conducted for a pure mode I loading scenario, however, in reality a pure mode I scenario does not always occur and the other two modes could exist at the same time. A mixed-mode scenario is the consequence of the combined relative effect of crack orientation, specimen geometry, and loading conditions. For the purpose of this paper, we will consider the mixed mode I and mode II loading conditions (Fig. 1).

Mixed-mode loading and T -stress play significant roles in fracture mechanics and yet their combined effects on the crack tip plastic zones have not been studied comprehensively. This paper will conduct the detail derivation of an expression for the plastic zone size that incorporates the effect of mixed mode I and mode II loading conditions and the T -stress. The resulting plastic zone will be plotted, and the results will be discussed.

2. CRACK-TIP PLASTIC ZONE ANALYSIS

2.1 Modeling the Plastic Zone

In two-parameter fracture mechanics using T-stress as a constraint parameter, the stress field around the crack-tip (Fig. 2) of a two-dimensional crack embedded in an isotropic linear elastic material subjected to mixed mode I and mode II plain-strain loading conditions is given by the following expressions [4]:

$$\sigma_{xx} = \frac{K_I}{\sqrt{2\pi r}} \cos\left(\frac{\theta}{2}\right) \left[1 - \sin\left(\frac{\theta}{2}\right) \sin\left(\frac{3\theta}{2}\right)\right] - \frac{K_{II}}{\sqrt{2\pi r}} \sin\left(\frac{\theta}{2}\right) \left[2 + \cos\left(\frac{\theta}{2}\right) \cos\left(\frac{3\theta}{2}\right)\right] + T \quad (1)$$

$$\sigma_{yy} = \frac{K_I}{\sqrt{2\pi r}} \cos\left(\frac{\theta}{2}\right) \left[1 + \sin\left(\frac{\theta}{2}\right) \sin\left(\frac{3\theta}{2}\right)\right] + \frac{K_{II}}{\sqrt{2\pi r}} \sin\left(\frac{\theta}{2}\right) \cos\left(\frac{\theta}{2}\right) \cos\left(\frac{3\theta}{2}\right) \quad (2)$$

$$\sigma_{zz} = \nu(\sigma_{xx} + \sigma_{yy}) = 2\nu \left\{ \frac{K_I}{\sqrt{2\pi r}} \cos\left(\frac{\theta}{2}\right) - \frac{K_{II}}{\sqrt{2\pi r}} \sin\left(\frac{\theta}{2}\right) \right\} + \nu T \quad (3)$$

$$\tau_{xy} = \frac{K_I}{\sqrt{2\pi r}} \sin\left(\frac{\theta}{2}\right) \cos\left(\frac{\theta}{2}\right) \cos\left(\frac{3\theta}{2}\right) + \frac{K_{II}}{\sqrt{2\pi r}} \cos\left(\frac{\theta}{2}\right) \left[1 - \sin\left(\frac{\theta}{2}\right) \sin\left(\frac{3\theta}{2}\right)\right] \quad (4)$$

$$\tau_{yz}, \tau_{zx} = 0 \quad (5)$$

where, (r, θ) are the polar coordinates and (x, y) are the Cartesian coordinates both with origins at the crack tip (Fig. 2). K_I and K_{II} are the mode I and mode II stress intensity factors (SIF) respectively, σ and τ are the normal and shear stress respectively, and ν is Poisson's ratio. The T term in Eq. (1) is the elastic T-stress, which under plane strain loading conditions induces a stress equivalent to νT in the z-direction, Eq. (3).

By definition, the plastic zone also known as the crack-tip-yielding zone is the region surrounding the crack tip that has yielded as a result of a localized stress field. In this case, the stress field is represented by Eqs. (1) – (5) for plane strain conditions. The plastic zone around a crack-tip can therefore be determined using the Von Mises yield criterion below [5]:

$$\left[(\sigma_{xx} - \sigma_{yy})^2 + (\sigma_{yy} - \sigma_{zz})^2 + (\sigma_{zz} - \sigma_{xx})^2 + 6(\tau_{xy}^2 + \tau_{yz}^2 + \tau_{zx}^2) \right] \leq 2\sigma_y^2 \quad (6)$$

where, σ_y is the material yield stress.

Use the condition represented by Eq. (6) and the stress fields from Eq. (1) to (5), the plastic zone size can be estimated. Specific cases of the plastic zone estimated can be found in Anderson [5] for single modes of fracture (mode I, II, and III) excluding the effect of T-stress. In addition, Kang and Beom [6] conducted the analysis for a constrained ductile layer. Gao et al [7] obtained the plastic zone for combined mode I and II loads. However, all those analyses have ignored the effect from T-stress in Eqs. (1) and (3).

In the present paper, the mixed-mode stress field, Eqs. (1) to (5), is substituted into the Von Mises yield criterion (6), and solved for the distance $r = r_p$ from the crack tip where the onset of yielding takes place. T-stress effect and mixed mode effects are considered together. After comprehensive mathematical manipulations, the solution for r_p as a function of θ is given by the following formula:

$$r_p(\theta) = \frac{1}{2\pi} \left(\frac{K}{\sigma_y} \right)^2 \left[\frac{1}{c^*} \left\{ [b]t_y - \sqrt{[b]^2 t_y^2 - [a]c^*} \right\} \right]^2 \quad (7)$$

The term r_p is the distance from the crack-tip where, for an applied stress field, the specimen begins to yield under static loading. The terms used in the right-hand side are defined as follows:

$$\text{The net SIF } K = \sqrt{K_I^2 + K_{II}^2} \quad (8)$$

$$\text{Phase angle } \phi = \tan^{-1} \frac{K_{II}}{K_I} \quad (9)$$

The net SIF K represents the net combined effect of the mode I and mode II SIF's on the crack-tip, while ϕ represents the phase angle separating the mode I and mode II SIF's where $\tan \phi$ denotes the mode II to mode I SIF ratio. Note, the boundary conditions of K and ϕ are $K = K_I$ at $\phi = 0^\circ$ for a pure mode I loading condition, and $K = K_{II}$ at $\phi = 90^\circ$ for a pure mode II loading condition.

$$\text{The normalized T-stress with respect to the yield stress } t_y = \frac{T}{\sigma_y} \quad (10)$$

The additional constants are:

$$c^* = [c]t_y^2 - 2 \quad (11)$$

$$[a] = \left[\cos^2 \phi \cdot \left\{ \frac{3}{2} \sin^2 \theta + V(\cos \theta + 1) \right\} + \cos \phi \cdot \sin \phi \cdot \left\{ 2 \sin \theta \cdot (3 \cos \theta - V) \right\} \right. \\ \left. + \sin^2 \phi \cdot \left\{ 6 - \frac{9}{2} \sin^2 \theta - V(\cos \theta - 1) \right\} \right] \quad (12)$$

$$[b] = \left[\cos \phi \cdot \left\{ \cos \frac{\theta}{2} \cdot \left(-3 \left\{ \cos^2 \frac{\theta}{2} - \cos^2 \theta \right\} + V \right) \right\} + \sin \phi \cdot \left\{ \sin \frac{\theta}{2} \cdot \left(-3 \left\{ \cos^2 \frac{\theta}{2} + \cos^2 \theta \right\} - V \right) \right\} \right] \quad (13)$$

$$[c] = \left[\frac{1}{2} \{3 + V\} \right] \quad (14)$$

$$V = (1 - 2\nu)^2 \quad (15)$$

Note that,

$$K_I = K \cos \phi \quad (16)$$

$$K_{II} = K \sin \phi \quad (17)$$

Looking at Eq. (7), for a given angle θ , the plastic zone is explicitly a function of K , ϕ , T , σ_y , θ and ν .

To determine the validity of the plastic zone model derived above, Equation (7) is applied to a pure mode I situation and a mixed-mode situation both without T-stress, and the results agree with published solutions of Anderson [5] and Gao et al [7], respectively.

2.2 Plastic Zone Results

The plastic zone was mapped and analyzed using the plastic zone model (Eq. 7) for a linear-elastic material with a Poisson's ratio of 0.3; a common value for steels. The plastic zone was analyzed for a wide range of mixed mode I and mode II loading conditions within the limits of the pure mode I and pure mode II loading conditions. The plastic zone was also analyzed for normalized T-stress, t_y , values ranging from -1 to +1.

For various net SIF and normalized T-stress values, plastic zones were mapped around the crack-front from $\theta = -180^\circ$ to $\theta = 180^\circ$ one degree at a time using the normalized form of Equation (7) below:

$$\frac{r_p(\theta)}{h} = \frac{1}{2} \left[\frac{1}{c^*} \left\{ [b]t_y - \sqrt{[b]^2 t_y^2 - [a]c^*} \right\} \right]^2 \quad (18)$$

where the term h is defined as:

$$h = \frac{1}{\pi} \left(\frac{K}{\sigma_y} \right)^2 \quad (19)$$

The plastic zones were mapped for mode II to mode I SIF ratios, Eq. (9) ranging from $\phi = 0^\circ$ to $\phi = 90^\circ$ in increments of 10° with normalized T-stress values ranging from $-1 \leq t_y \leq 1$ in increments of 0.25. The SIF ratios of $\phi = 0^\circ$ and $\phi = 90^\circ$ represent the pure mode I and pure mode II cases respectively, and therefore all SIF ratios between these two limits represent mixed-mode conditions. Maps of the plastic zones can be viewed in Figures 3(a) to 3(i). Note only typical results for $\phi = 60^\circ$ are shown in these figures.

The range of the normalized T-stress t_y was chosen to be within the limits of ± 1 for the reason that none of the stresses (including the T-stress) within the region of the plastic zone can exceed the yield stress before yielding occurs.

The plastic zones are mapped with the Cartesian coordinate system using the following polar to Cartesian conversions:

$$x_p = r_p(\theta) \cdot \cos \theta \quad (20)$$

$$y_p = r_p(\theta) \cdot \sin \theta \quad (21)$$

Note that in Figure 3 the cracks emanate from the left-hand-side of the graphs with the crack-tips located at the origin in the center of the graph. It is clear that the general shape and size of the plastic zone vary with the normalized T-stress, t_y . Although not shown here, the plastic zones also vary with different ϕ values.

3. DISCUSSIONS

3.1 Continuity of Plastic Zone Boundary

From the plastic zone maps (Fig. 3), it is observed that only one of the maps have a continuous plastic zone boundary while the rest of the maps exhibit a discontinuity in the plastic zone boundary across the crack-front i.e. at $\theta = \pm 180^\circ$.

This effect is more significant for large T-stress values. To investigate the nature of the plastic zone boundary across the crack-front, expressions for the yield points at $\theta = -180^\circ$ and $\theta = +180^\circ$ were formulated in the same way as Equation (7) and subtracted from each other. The resulting expression for the plastic zone boundary across the crack-front is found as below:

$$r_p(\theta=180) - r_p(\theta=-180) = \frac{-8 \left(\frac{K_{II}}{\sigma_y} \right)^2 t_y W^{3/2}}{\pi \left\{ t_y^2 W - 1 \right\}^2} \quad (22)$$

where, $W = \{\nu^2 - \nu + 1\}$.

The nature of the plastic zone boundary across the crack-front has clearly been determined by Eq. (22). From the expression, it can be noted that the plastic zone boundary is continuous i.e. $r_p(\theta=180) - r_p(\theta=-180) = 0$ if at least one of the following two conditions are met:

i). $K_{II} = 0$

That is, discontinuous plastic zone boundaries are possible only under pure mode II and mixed mode I and mode II loading conditions, while continuous plastic zone boundaries exist under pure mode I loading conditions.

ii) $t_y = 0$

Or, discontinuous plastic zone boundaries are possible only when the T-stress is not zero, while continuous plastic zone boundaries exist when the T-stress is zero, as shown in Figure 3(e).

Summarizing, the conditions necessary for a continuous plastic zone boundary are a pure mode I loading condition and/or a zero T-stress, while the conditions necessary for a discontinuous plastic zone boundary is a loading condition involving a mode II component (either wholly or partially) combined with a non-zero T-stress.

3.2 Maximum Plastic Zone Size

For any given plastic zone, the maximum size $r_{p \max}$ is the most critical value characterizing that plastic zone. The maximum plastic zone size (PZS) was determined in its normalized form $r_{p \max} / h$ by first calculating the PZS one degree at a time from $\theta = -180^\circ$ to $\theta = 180^\circ$ using Equation (18) and then manually identifying the maximum value. The values of the maximum PZS are obtained.

The maximum PZS, its variation with the normalized T-stress for various phase angles is plotted in Figure 4. The variation of $r_{p \max} / h$ as a function of the normalized T-stress can be observed.

From Figure 4, the general trend of the maximum PZS versus normalized T-stress follows a squared-U-path. The maximum PZS drops sharply from $t_y = -1$ to $t_y = -0.75$ followed by a steady drop from $t_y = -0.75$ to $t_y = 0$. The maximum PZS then shows a steady increase from $t_y = 0$ to $t_y = 0.75$ followed by a sharp increase from $t_y = 0.75$ to $t_y = 1$.

Referring to Figure 5, the magnitude of the maximum PZS increases with ϕ at a given T-stress are plotted ($t_y = 0$ case shown here). The largest and

smallest values of the maximum PZS are associated with $\phi = 90^\circ$ (pure mode II) and $\phi = 0^\circ$ (pure mode I), respectively. Same trends are observed for non-zero T-stress cases.

It is clear from Figures 3-5 that the plastic zone size is affected by T-stress for mixed mode loading conditions, and the effect is even more significant for predominantly mode II conditions.

4. CONCLUSIONS

This paper has examined the plastic zone variation under mixed mode loading conditions influenced by T-stress. Plane strain conditions are considered. An expression was developed for the plastic zone variation for various combinations of mode II to mode I SIF ratios and T-stress levels. The plastic zones were mapped and plotted. The following conclusions are summarised:

1). The plastic zones are affected by a variety of factors including the net stress intensity factor K , the mixed mode phase angle, ϕ and the T-stress level, $t_y = \frac{T}{\sigma_y}$. The T-stress plays a very important role in the plastic zone size variations. The plastic zone size is significantly larger for mode II dominant conditions.

2). It is observed that under the presence of T-stress and mixed mode loading, the plastic zone will have a discontinuity across the crack face. The condition for the plastic zone to be continuous across the crack face are either the $K_{II} = 0$ or $t_y = 0$.

3). Further studies are recommended to study the effect of T-stress on fracture initiation and fatigue crack propagation under mixed mode loading conditions.

Acknowledgements

The authors gratefully acknowledge the financial supports from the Natural Sciences and Engineering Research Council (NSERC) of Canada and Ontario Centres of Excellence (OCE).

REFERENCES

- [1] J.R. Rice, "Limitations to the small scale yielding approximation for crack tip plasticity", *Journal of the Mechanics and Physics of Solids*, Vol. 22, (1974), pp. 17-26.
- [2] Z.Z. Du & J.W. Hancock, "The effect of non-singular stresses on crack-tip constraint", *Journal of the Mechanics and Physics of Solids*, Vol. 39, (1991) pp. 555-567.
- [3] M.R. Ayatollahi, M.J. Pavier, & D.J. Smith, "Determination of T-stress from finite element analysis for mode I and mixed mode I/II loading", *International Journal of Fracture*, Vol. 91, (1998), pp. 283-298.
- [4] M.L. Williams, "On the stress distribution at the base of a stationary crack", *ASME Journal of Applied Mechanics*, Vol. 24, (1957), pp. 109-114.
- [5] T.L. Anderson, *Fracture Mechanics: Fundamentals and Applications* (3rd

Ed.), Taylor & Francis Group, 2005.

[6] K.J. Kang & H.G. Beom, "Plastic zone size near the crack tip in a constrained ductile layer under mixed mode loading", *Engineering Fracture Mechanics*, Vol. 66, (1991), pp. 257-268.

[7] H. Gao, N. Alagok, M.W. Brown, & K.J. Miller, "Growth of fatigue cracks under combined mode I and mode II loads", *Multiaxial Fatigue, ASTM STP 853*, K.J. Miller & M.W. Brown, Eds., American Society for Testing and Materials, (1985), pp. 184-202.

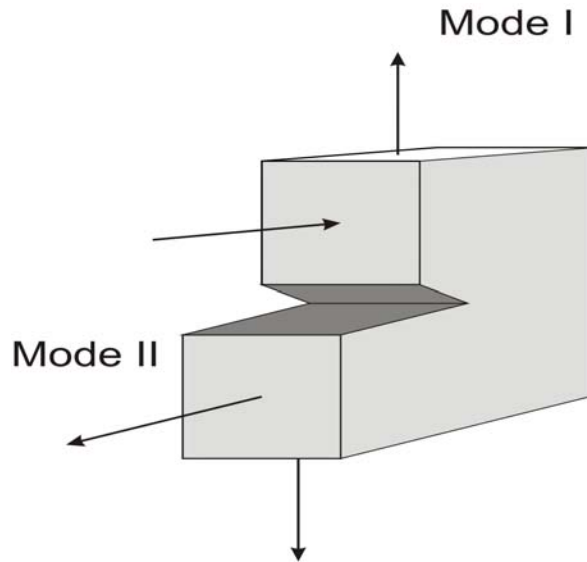


Figure 1 Mixed mode I and mode II fracture

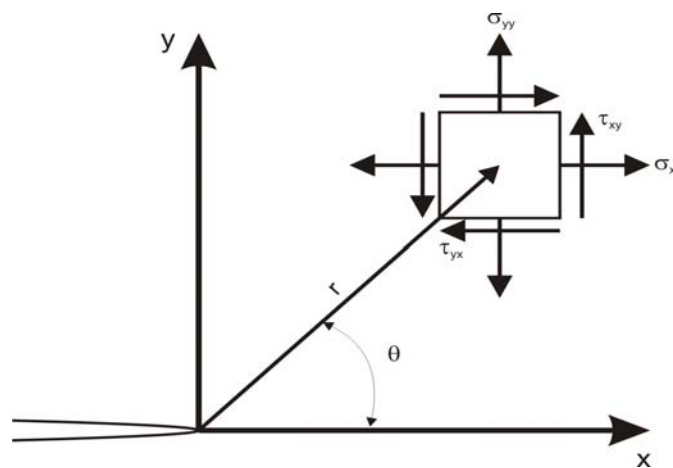
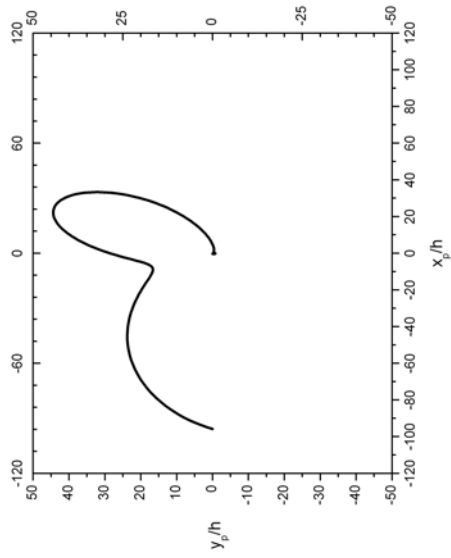
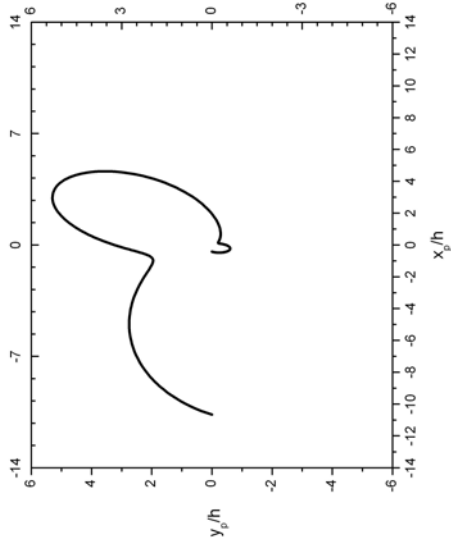


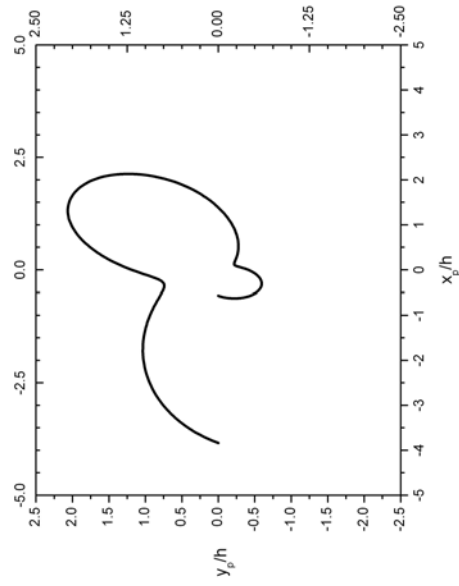
Figure 2 Definition of the coordinate axis around the crack-tip



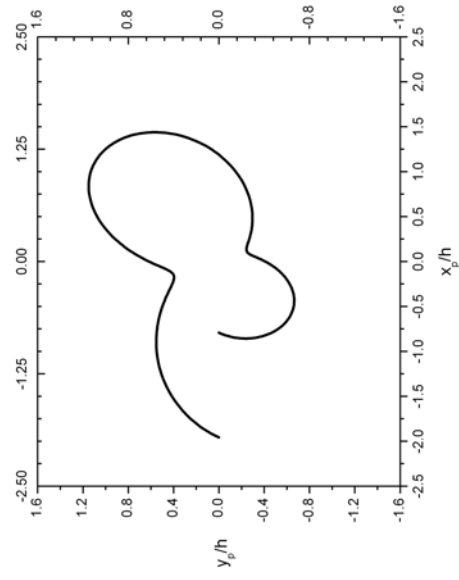
(a) $t_y = -1$



(b) $t_y = -0.75$

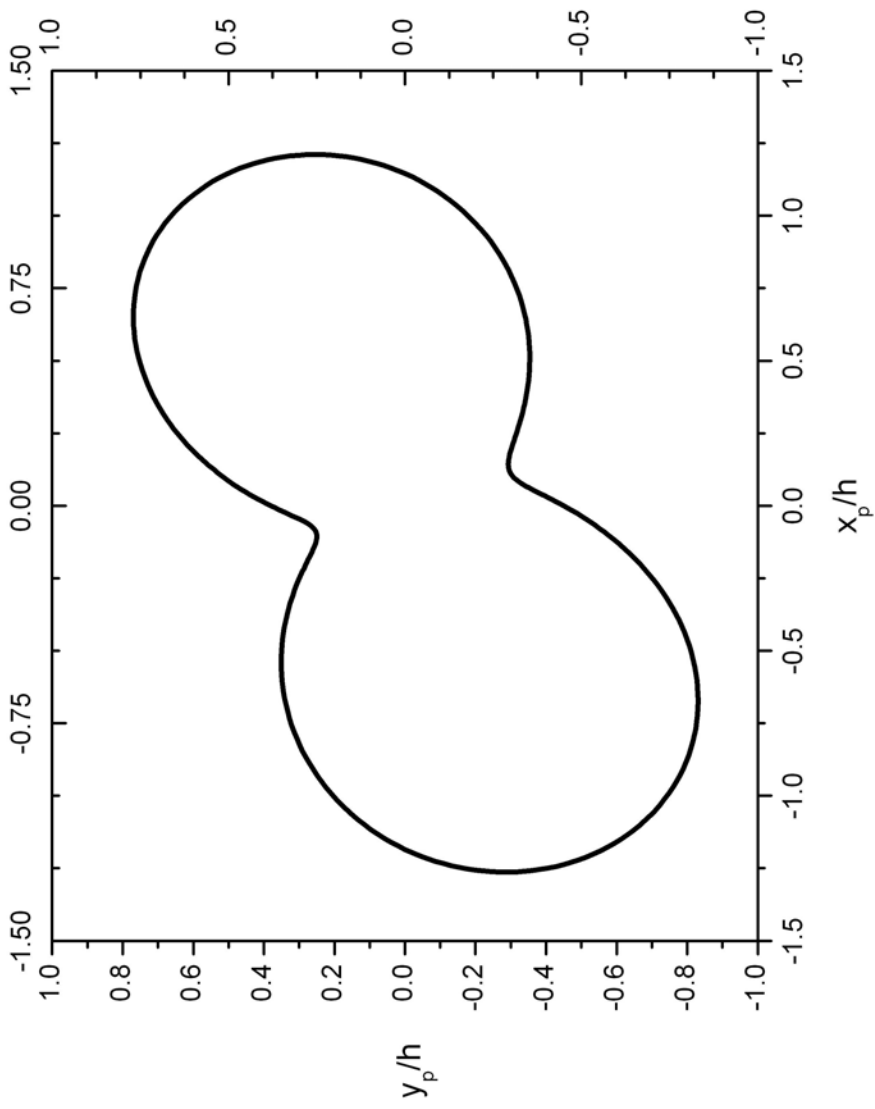


(c) $t_y = -0.5$



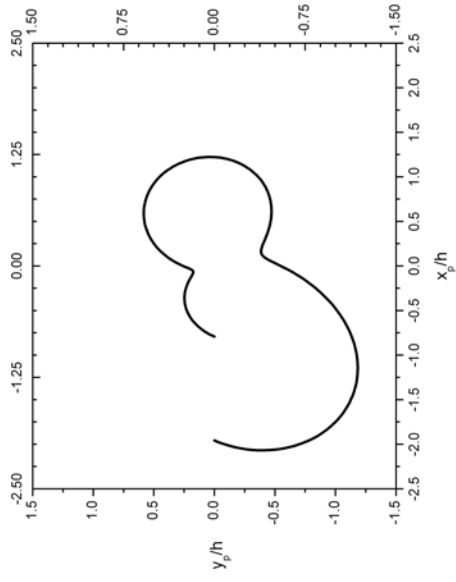
(d) $t_y = -0.25$

Figure 3: Plastic zone maps for $\phi = 60^\circ$ (a)-(d)



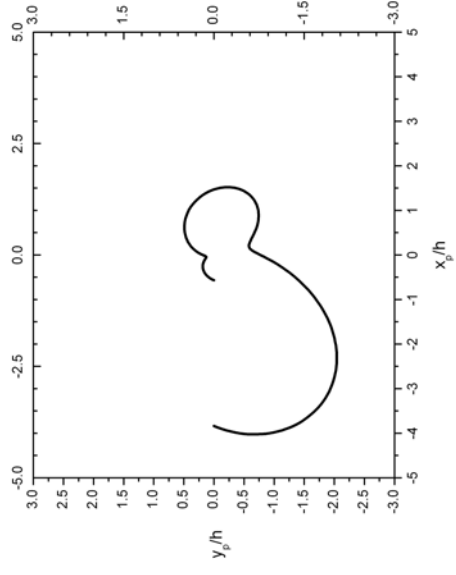
(e) $t_{ij}=0$

Figure 3: Plastic zone maps for $\phi = 60^\circ$ (e)

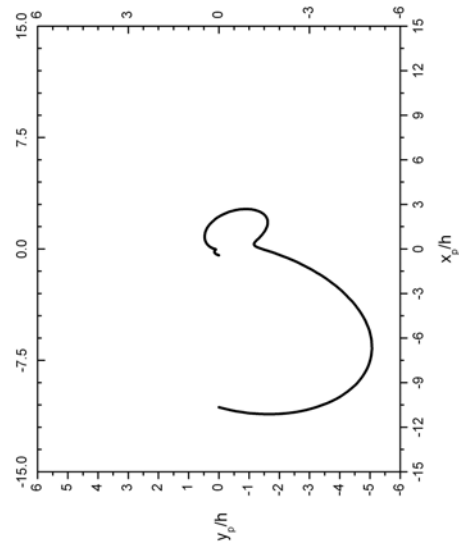


10

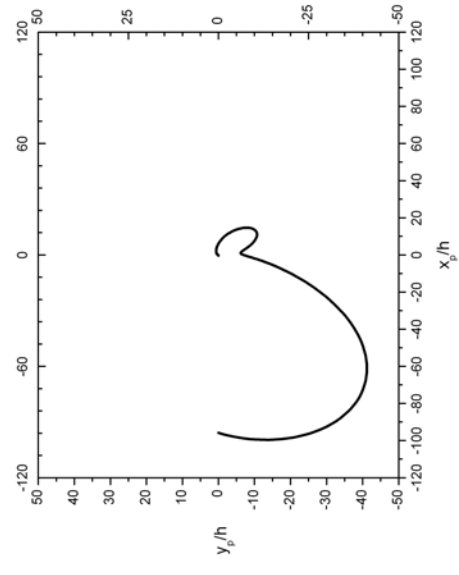
(g) $t_y=0.5$



(h) $t_y=0.75$



(i) $t_y=1$



(f)-(i)

Figure 3: Plastic zone maps for $\phi = 60^\circ$ (f)-(i)

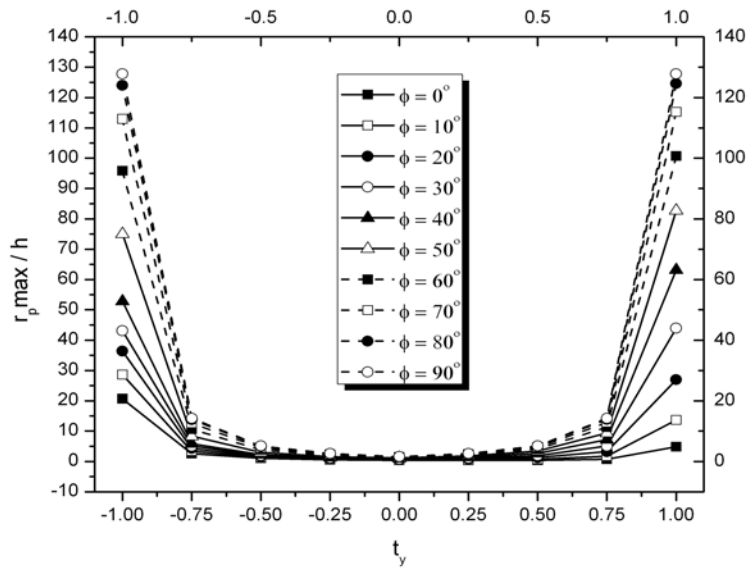


Figure 4 Combined graphs of maximum plastic zone size as a function of the normalized T-stress ($-1 \leq t_y \leq 1$) for various phase angles

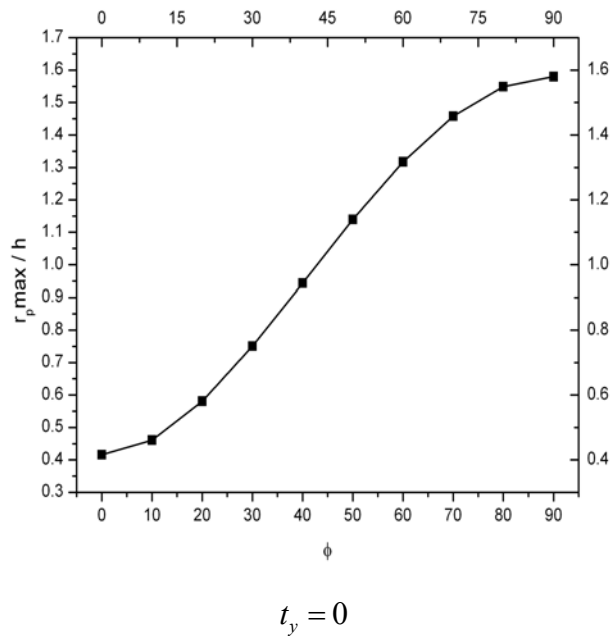


Figure 5 Graphs of maximum plastic zone size as a function of phase angle for T-stress value $t_y = 0$